Journal of Applied Physics & Nanotechnology

(ISSN 2638-5104)

Research Article

On the Equality of Electric Power Fractal Dimension and Capillary Pressure Fractal Dimension for Characterizing Shajara Reservoirs of the Permo-Carboniferous Shajara Formation

This article was published in the following Scient Open Access Journal:
Journal of Applied Physics & Nanotechnology

Received February 12, 2019; **Accepted** February 25, 2019; **Published** March 04, 2019

Prof. Khalid Elyas Mohamed Elameen Alkhidir, Ph.D.*

Department of Petroleum and Natural Gas Engineering, College of Engineering King Saud University, Saudi Arabia

Abstract

The quality and assessment of a reservoir can be documented in details by the application of electric power. This research aims to calculate fractal dimension from the relationship among electric power, maximum electric power and wetting phase saturation (water saturation) and to confirm it by the fractal dimension derived from the relationship among capillary pressure and wetting phase saturation (water saturation). In this research, porosity was measured on real collected sandstone samples and permeability was calculated theoretically from capillary pressure profile measured by mercury intrusion techniques. Two equations for calculating the fractal dimensions have been employed. The first one describes the functional relationship between wetting phase saturation, electric power, maximum electric power and fractal dimension. The second equation implies to the wetting phase saturation as a function of capillary pressure and the fractal dimension. Two procedures for obtaining the fractal dimension have been utilized. The first procedure was done by plotting the logarithm of the ratio between electric power and maximum electric power versus logarithm wetting phase saturation. The slope of the first procedure is positive = 3- Df (fractal dimension). The second procedure for obtaining the fractal dimension was completed by plotting logarithm of capillary pressure versus the logarithm of wetting phase saturation. The slope of the second procedure is negative = Df -3. On the basis of the obtained results of the fabricated stratigraphic column and the attained values of the fractal dimension, the sandstones of the Shajara reservoirs of the Shajara Formation were divided here into three units. These units from bottom to top are: Lower Shajara Electric power Fractal Dimension Unit, Middle Shajara Electric power Fractal Dimension Unit, Upper Shajara Electric power Fractal Dimension Unit. The three reservoir units were also confirmed by capillary pressure fractal dimension. It was found that the obtained fractal dimension increases with increasing grain size and permeability.

Keywords: Shajara Reservoirs, Shajara Formation, Electric power fractal dimension, Capillary pressure fractal dimension

Introduction

Toledo et al. [1] reported that the wetting phase saturation can be described as function of capillary pressure and fractal dimension. Li and Horne [2] demonstrated that the Purcell model was found to be the best fit to the experimental data of the wetting phase relative permeability for the cases as long as the measured capillary pressure curve had the same residual saturation as the relative permeability curve. They also reported that in the reverse procedure, capillary pressure could also be computed once relative permeability data are available. Li and Willams [3] derived theoretically a model to correlate capillary pressure and resistivity index based on the fractal scaling theory. Their results demonstrated that the model could match the experimental data in a specific range of low water saturation. Zhang and Weller [4] showed the fractal dimension resulting from longer transverse NMR relaxation times and lower capillary pressure reflects the volume dimension of larger pores. They also reported that the fractal dimension derived from the short NMR relaxation times is similar to the fractal dimension of the internal surface. Wang et al [5] reported that the fractal dimensions can be used to represent the complexity degree and heterogeneity of pore structure, and the coexistence of dissolution pores and large intergranular pores of Donghetang sandstones contributes to a heterogeneous pore throat distribution and a high value of fractal dimension. Guo, et al. [6] studied the relationship among capillary pressure (PC), nuclear magnetic transverse relaxation time (T2) and resistivity index (I). An increase of bubble pressure fractal dimension and pressure head fractal dimension and decreasing pore size distribution index and fitting parameters m * n due to possibility of having interconnected channels was confirmed by Al-khidir [7,8] An increase of fractal dimension with increasing arithmetic, geometric relaxation time of induced polarization, permeability and grain size was investigated by Alkhidir [9-11]. An

***Corresponding Author:** Khalid Elyas Mohamed Elameen Alkhidir, Department of Petroleum and Natural Gas Engineering, College of Engineering, King Saud University, Saudi Arabia
Tel: +966114679118, Email: kalkhidir@ksu.edu.sa

increase of seismo electric field and resistivity fractal dimensions with increasing permeability and grain size was described by Alkhidir [12-14]. An increase of electro kinetic fractal dimension with increasing permeability and grain size was reported by Alkhidir [15].

Material and Method

Samples were collected from the surface type section of the Shajara reservoirs of the Permo-carboniferous Shajara formation at latitude 26 ° 52′ 17.4″, longitude 43 ° 36′ 18″. Porosity was measured and permeability was derived from the measured capillary pressure data.

The electric power can be scaled as

$$Sw = \left[\frac{P}{P_{max}}\right]^{[3-Df]} \quad 1$$

Where Sw the water saturation, P the electric power in watt, Pmax the maximum electric power in watt, and Df the fractal dimension.

Equation 1 can be proofed from

$$J = \sigma * E \quad 2$$

Where J the electric current density in ampere / square meter, σ the electric conductivity in Siemens / meter. and E the electric field volt / meter.

But the electric conductivity σ can be scaled as

$$\sigma = \left[\frac{2 * \Sigma}{r}\right] \quad 3$$

Where Σ the surface conductance in Siemens, and r the grain radius in meter.

$$J = \left[\frac{2 * \Sigma * E}{r}\right] \quad 4$$

The electric field E can be scaled as

$$E = \left[\frac{V}{L}\right] \quad 5$$

Where V the electric potential in volt, and L the distance in meter.

Insert Equation 5 and Equation 4.

$$J = \left[\frac{2 * \Sigma * V}{r * L}\right] \quad 6$$

$$V = \left[\frac{U}{Q}\right] \quad 7$$

Where U the electric potential energy in Joule, and Q the electric charge in Coulomb.

Insert equation 7 into Equation 6.

$$J = \left[\frac{2 * \Sigma * U}{r * L * Q}\right] \quad 8$$

The electric potential energy U can be scaled as

$$U = P * t \quad 9$$

Where P the electric power in watt and t the time in second.

Insert equation 9 into Equation 8

$$J = \left[\frac{2 * \Sigma * P * t}{r * L * Q}\right] \quad 10$$

Equation 10 after rearrange of grain radius r will become

$$r = \left[\frac{2 * \Sigma * P * t}{J * L * Q}\right] \quad 11$$

The maximum grain radius rmax can be scaled as

$$r_{max} = \left[\frac{2 * \Sigma * P_{max} * t}{J * L * Q}\right] \quad 12$$

$$\left[\frac{r}{r_{max}}\right] = \left[\frac{\left[\frac{2 * \Sigma * P * t}{J * L * Q}\right]}{\left[\frac{2 * \Sigma * P_{max} * t}{J * L * Q}\right]}\right] \quad 13$$

Equation 13 after simplification will become

$$\left[\frac{r}{r_{max}}\right] = \left[\frac{P}{P_{max}}\right] \quad 14$$

Take the logarithm of Equation 14

$$\log\left[\frac{r}{r_{max}}\right] = \log\left[\frac{P}{P_{max}}\right] \quad 15$$

$$\text{But, } \log\left[\frac{r}{rmax}\right] = \frac{\log Sw}{[3 - Df]} \quad 16$$

Insert equation 16 into Equation 15

$$\frac{\log Sw}{[3 - Df]} = \log\left[\frac{P}{Pmax}\right] \quad 17$$

Equation 17 after log removal will become

$$Sw = \left[\frac{P}{Pmax}\right]^{[3-Df]} \quad 18$$

Equation 18 the proof of equation 1 which relates the water saturation Sw, the electric power P, the maximum electric power Pmax , and the fractal dimension Df.

The capillary pressure can be scaled as

$$\log Sw = (Df - 3) * \log Pc + constant \quad 19$$

Where Sw the water saturation, Pc the capillary pressure and Df the fractal dimension

Result and Discussion

Based on field observation the Shajara Reservoirs of the Permo-Carboniferous Shajara Formation were divided here into three units as designated in Figure 1. These units from bottom to top are: Lower Shajara Reservoir, Middle Shajara reservoir, and Upper Shajara Reservoir. Their developed results of the electric power fractal dimension and capillary pressure fractal

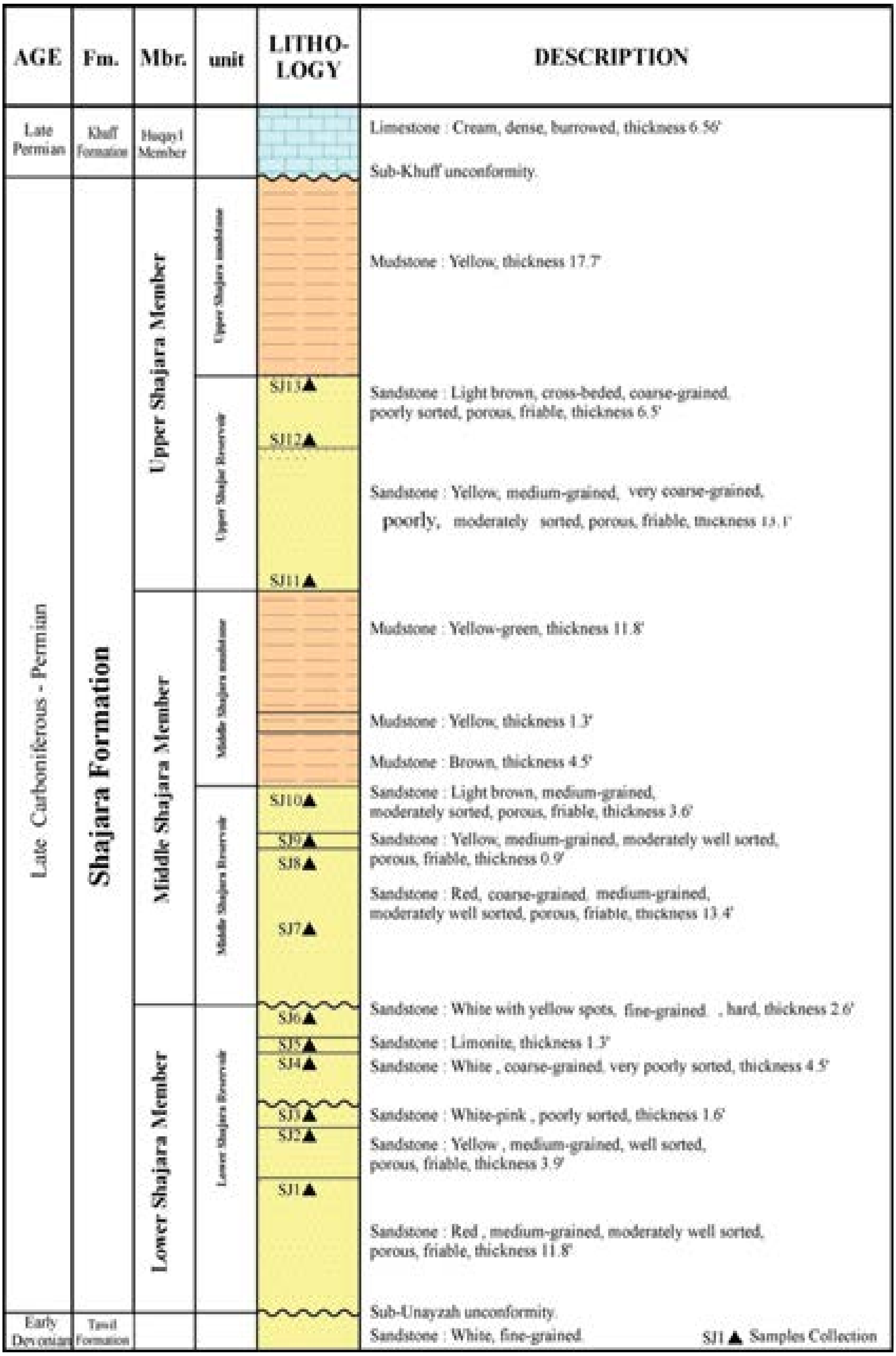

Figure 1: Surface type section of the Shajara reservoirs of the Permo-Carboniferous Shajara Formation at latitude 26° 52' 17.4", longitude 43° 36' 18".

dimension are shown in Table 1. Based on the achieved results it was found that the electric power fractal dimension is equal to the capillary pressure fractal dimension. The maximum value of the fractal dimension was found to be 2.7872 assigned to sample SJ13 from the Upper Shajara Reservoir as confirmed in Table 1. Whereas the minimum value 2.4379 of the fractal dimension was recounted from sample SJ3 from the Lower Shajara reservoir as displayed in Table 1. The electric power fractal dimension and capillary pressure fractal dimension were witnessed to increase with increasing permeability as proofed in (Table 1) owing to the possibility of having interconnected channels.

The Lower Shajara reservoir was symbolized by six sandstone samples (Figure 1), four of which considered as SJ1, SJ2, SJ3 and SJ4 as confirmed in Table 1, were carefully chosen for capillary pressure measurement. Their positive slopes of the first procedure and negative slopes of the second procedure are delineated in Figures 2-5 and Table 1. Their electric power fractal dimension and capillary pressure fractal dimension values are proofed in Table 1. As we proceed from sample SJ2 to SJ3 a pronounced reduction in permeability due to compaction was reported from 1955 md to 56 md which reflects decrease in electric power fractal dimension and capillary pressure fractal dimension from 2.7748 to 2.4379 as specified in Table 1. Again, an increase in grain size and permeability was recorded from sample SJ4 whose electric power fractal dimension and capillary pressure fractal dimension was found to be 2.6843 as described in Table 1.

In contrast, the Middle Shajara reservoir which is separated from the Lower Shajara reservoir by an unconformity surface as shown in Figure 1. It was designated by four samples (Figure 1), three of which named as SJ7, SJ8, and SJ9 as illustrated in Table 1, were picked for capillary pressure measurement. Their positive slopes of the first procedure and negative slopes of the second procedure are displayed in Figures 6-8 and Table 1. Their electric power fractal dimensions and capillary pressure fractal dimensions show similarities as defined in Table 1. Their fractal dimensions are higher than those of samples SJ3 and SJ4 from the Lower Shajara Reservoir due to an increase in their permeability as elucidated in Table 1.

On the other hand, the Upper Shajara reservoir is separated

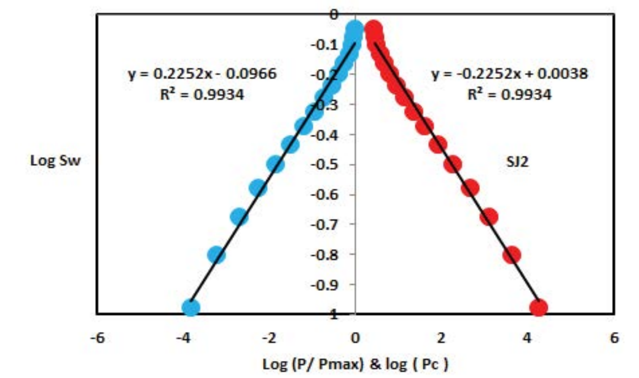

Figure 3: Log (P / Pmax) & log (Pc) versus log Sw for sample SJ2

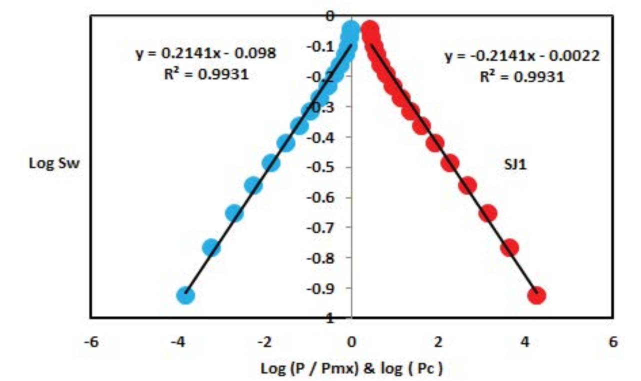

Figure 2: Log (P / Pmax) & log (Pc) versus log Sw for sample SJ1

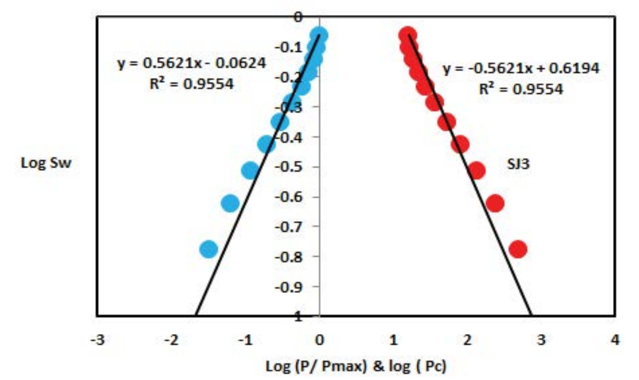

Figure 4: Log (P / Pmax) & log (Pc) versus log Sw for sample SJ3

Table 1: Petrophysical model showing the three Shajara Reservoir Units with their corresponding values of electric power fractal dimension and capillary pressure fractal dimension

Formation	Reservoir	Sample	Porosity %	k (md)	Positive slope of the first procedure Slope=3-Df	Negative slope of the second procedure Slope=Df-3	Electric power fractal dimension	Capillary pressure fractal dimension
Permo-Carboniferous Shajara Formation	Upper Shajara Reservoir	SJ13	25	973	0.2128	-0.2128	2.7872	2.7872
		SJ12	28	1440	0.2141	-0.2141	2.7859	2.7859
		SJ11	36	1197	0.2414	-0.2414	2.7586	2.7586
	Middle Shajara Reservoir	SJ9	31	1394	0.2214	-0.2214	2.7786	2.7786
		SJ8	32	1344	0.2248	-0.2248	2.7752	2.7752
		SJ7	35	1472	0.2317	-0.2317	2.7683	2.7683
	Lower Shajara Reservoir	SJ4	30	176	0.3157	-0.3157	2.6843	2.6843
		SJ3	34	56	0.5621	-0.5621	2.4379	2.4379
		SJ2	35	1955	0.2252	-0.2252	2.7748	2.7748
		SJ1	29	1680	0.2141	-0.2141	2.7859	2.7859

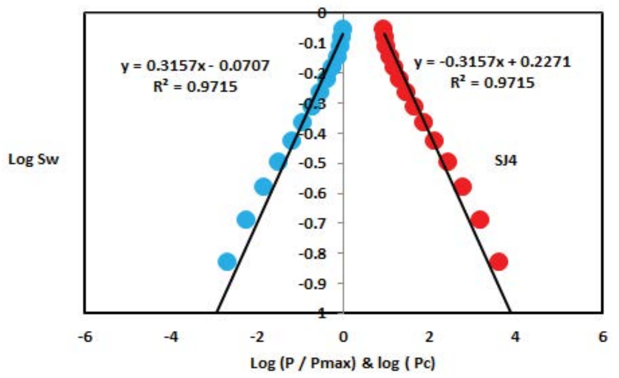

Figure 5: Log (P / Pmax) & log (Pc) versus log Sw for sample SJ4

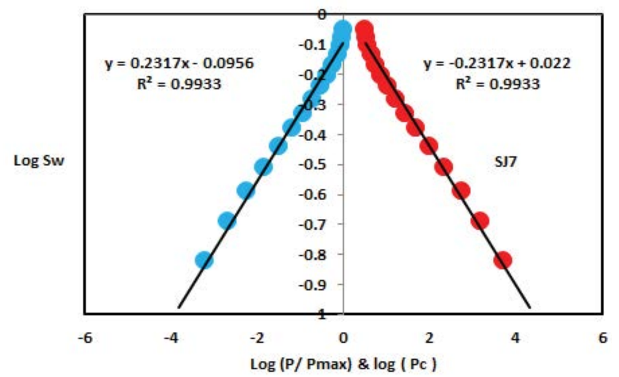

Figure 6: Log (P / Pmax) & log (Pc) versus log Sw for sample SJ7

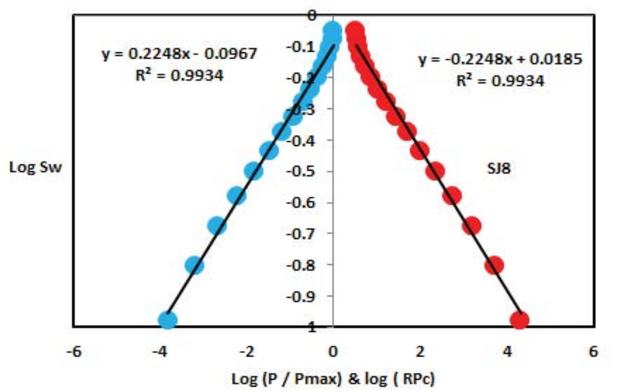

Figure 7: Log (P / Pmax) & log (Pc) versus log Sw for sample SJ8

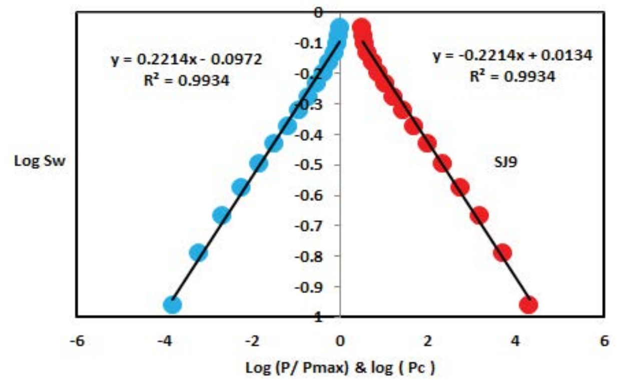

Figure 8: Log (P / Pmax) & log (Pc) versus log Sw for sample SJ9

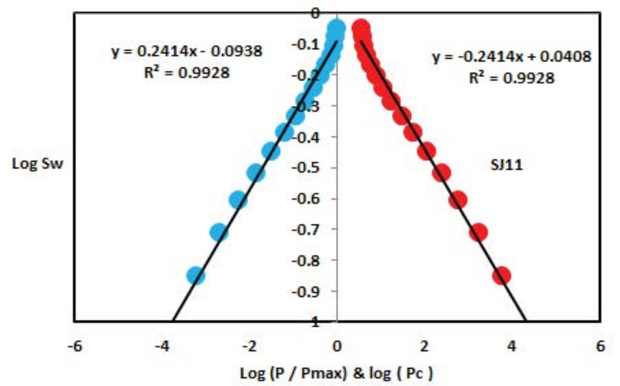

Figure 9: Log (P / Pmax) & log (Pc) versus log Sw for sample SJ11

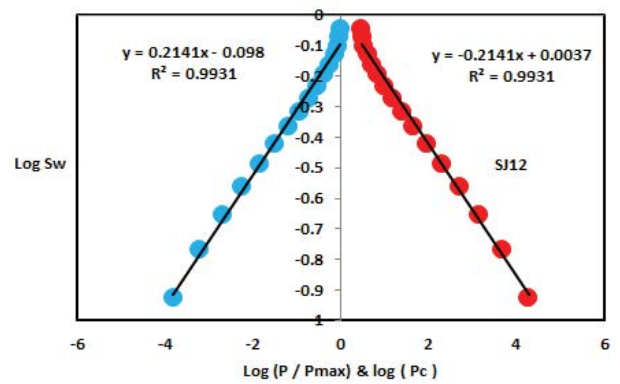

Figure 10: Log (P / Pmax) & log (Pc) versus log Sw for sample SJ12

from the Middle Shajara reservoir by yellow green mudstone as revealed in Figure 1. It is defined by three samples so called SJ11, SJ12, SJ13 as explained in Table 1. Their positive slopes of the first procedure and negative slopes of the second procedure are exhibited in Figures 9-11 and Table 1. Moreover, their electric power fractal dimension and capillary pressure fractal dimension are also higher than those of sample SJ3 and SJ4 from the Lower Shajara Reservoir due to an increase in their permeability as explained in Table 1.

Overall a plot of electric power fractal dimension versus capillary pressure fractal dimension as shown in Figure 12, reveals three permeable zones of varying Petrophysical properties. Such variation in fractal dimension can account for heterogeneity which is a key parameter in reservoir quality assessment. This heterogeneity was also confirmed by plotting positive slopes of the first procedure versus negative slopes of the second procedure as proofed in Figure 13.

Conclusion

The sandstones of the Shajara Reservoirs of the Permo-Carboniferous Shajara Formation were divided here into three

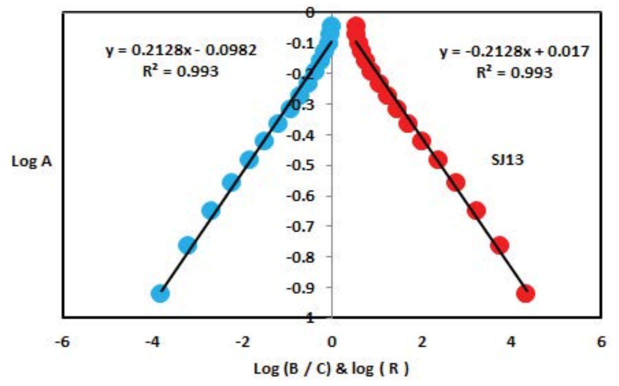

Figure 11: Log (P / Pmax) & log (Pc) versus log Sw for sample SJ13

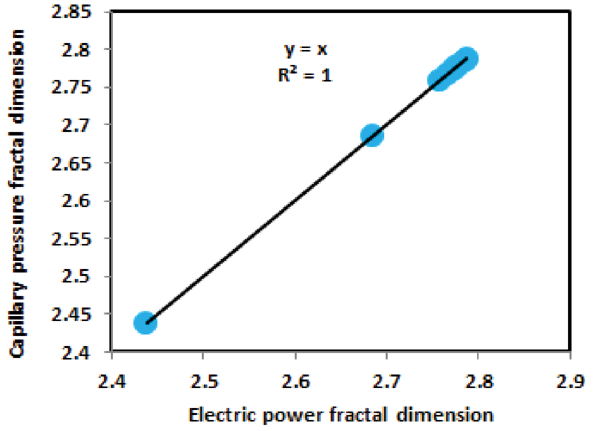

Figure 12: Electric power fractal dimension versus capillary pressure fractal

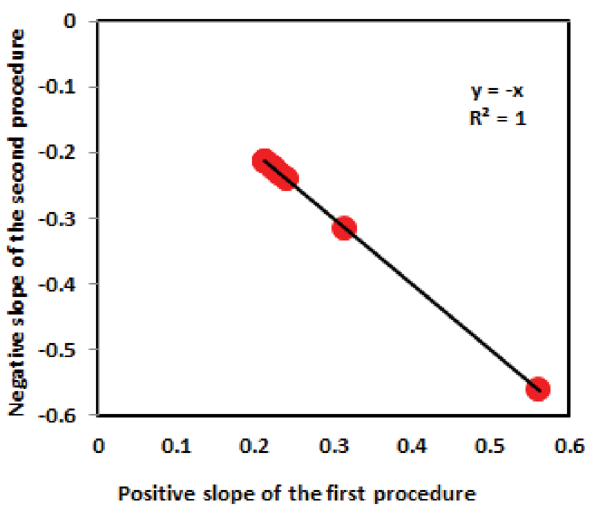

Figure 13: Positive slope of the first procedure versus negative slope of the second procedure

units based on electric power fractal dimension. The Units from bottom to top are: Lower Shajara Electric Power Fractal dimension Unit, Middle Shajara Electric Power Fractal Dimension Unit, and Upper Shajara Electric power Fractal Dimension Unit. These units were also proved by capillary pressure fractal dimension. The fractal dimension was found to increase with increasing grain size and permeability.

Acknowledgement

The author would like to thank King Saud University, College of Engineering, Department of Petroleum and Natural Gas Engineering, Department of Chemical Engineering, Research Centre at College of Engineering, and King Abdullah Institute for Research and Consulting Studies for their supports.

References

1. Toledo P G, Navy R A, Davis H T, Scriven L E. Capillary pressure, water relative permeability, electrical conductivity and capillary dispersion coefficient of fractal porous media at low wetting phase saturation, *23675-PA SPE Journal Paper*. 1994; 2(1):136-141.
2. Li K, Horne RN. Experimental verification of methods to calculate relative permeability using capillary pressure data. *76757-MS SPE Conference Paper*. 2002.
3. Li K, Willams W. Determination of capillary Pressure function from resistivity data. *Transport in Porous Media*. 2007;67:1-15.
4. Zhang Z, Weller A. Fractal Dimension of Pore-Space Geometry of Eocene sandstone Formation. *GEOPHYSICS*. 2014;79(6): D377-D387.
5. Wang Z, Pan M, Shi Y, Liu L, Xiong F, Qin Z. Fractal analysis of Donghetang sandstones using NMR measurements. *Energy Fuels*. 2018;32(3):2973-2982.
6. Guo Y-h, Pan B-z, Zhang L-h, Fang C-h. Research and application of the relationship between transverse relaxation time and resistivity index in tight sandstone reservoir. *Journal of petroleum science and engineering*. 2018;160:597-604.
7. Al-Khidir KEME. Pressure head fractal dimension for characterizing Shajara Reservoirs of the Shajara Formation of the Permo-Carboniferous Unayzah Group, Saudi Arabia.*Archives of Petroleum and Environmental Biotechnology*. 2017.
8. Al-Khidir KE. On Similarity of Pressure Head and Bubble Pressure Fractal Dimensions for Characterizing Permo-Carboniferous Shajara Formation, Saudi Arabia. *Journal of Industrial Pollution and Toxicity*. 2018;1(1).
9. Alkhidir KEME. Arithmetic relaxation time of induced polarization fractal dimension for characterizing Shajara Reservoirs of the Shajara Formation. *Nanoscience and Nanotechnology*. 2018;2(1):1-8.
10. Alkhidir KEME. Geometric relaxation time of induced polarization fractal dimension for characterizing Shajara Reservoirs of the Shajara formation of the Permo- Carboniferous Unayzah Group-Permo. *International Journal of Petrochemistry and Research*. 2018;2(1):105-108.
11. Alkhidir KEME. Geometric relaxation time of induced polarization fractal dimension for characterizing Shajara Reservoirs of The Shajara Formation of the Permo- Carboniferous Unayzah Group, Saudi Arabia, *SciFed Journal of Petroleum*. 2018; 2(1):1-6.
12. AlKhidir KEME. Seismo Electric field fractal dimension for characterizing Shajara Reservoirs of the Permo-Carboniferous Shajara Formation,Saudi Arabia.*Petroleum & Petrochemical Engineering Journal*. 2018;2(4).
13. Alkhidir KEME. Seismo electric field fractal dimension for characterizing Shajara reservoirs of the Permo-Carboniferous Shajara Formation,Saudi Arabia. *Academia Journal of Environmental Science*. 2018;6(5):113-120.
14. Alkhidir KEME. Resistivity Fractal Dimension for Characterizing Shajara Reservoirs of the Permo Carboniferous Shajara Formation, Saudi Arabia. *Recent Advances in Petrochemical Science*. 2018;5(2):1-6.
15. Alkhidir KEME. Electro Kinetic Fractal Dimension for Characterizing Shajara Reser voirs of the Permo-Carboniferous Shajara Formation, Saudi Arabia. *Archives of Oil and Gas Research*. 2018;2018(1):1-7.